Advances in Materials Physics and Chemistry, **2013, 3, 101-107**
http://dx.doi.org/10.4236/ampc.2013.31A012 Published Online April 2013 (http://www.scirp.org/journal/ampc)

XRD Characterization of AlN Thin Films Prepared by Reactive RF-Sputter Deposition

N. Matsunami[1], H. Kakiuchida[2], M. Sataka[3], S. Okayasu[3]
[1]Energy Science Division, EcoTopia Science Institute, Nagoya University, Nagoya, Japan
[2]National Institute of Advanced Industrial Science and Technology (AIST), Nagoya, Japan
[3]Japan Atomic Energy Agency (JAEA), Tokai, Japan
Email: n-matsunami@nucl.nagoya-u.ac.jp

Received January 22, 2013; revised March 10, 2013; accepted April 18, 2013

ABSTRACT

AlN thin films have been grown on R((1-12) surface-cut)-Al_2O_3, SiO_2-glass and C((001) surface-cut)-Al_2O_3 substrates, by using a reactive-RF-sputter-deposition method. X-ray diffraction (XRD) shows that AlN film has (110) orientation of wurtzite crystal structure for R-Al_2O_3 and (001) orientation for SiO_2-glass and C-Al_2O_3 substrates. The film thickness was analyzed by Rutherford backscattering spectroscopy (RBS) and it appears that XRD intensity does not show a linear increase with the film thickness but a correlation with the stress, *i.e*., deviation of the lattice parameter of the film from that of bulk. The film composition and impurities have been analyzed by ion beam techniques. Effects of high-energy ion beams are briefly presented on atomic structure (whether stress relaxation occurs or not), surface morphology and optical properties.

Keywords: Aluminum Nitride Film; Composition; Impurities; Atomic Structure; Surface Morphology; Optical Properties

1. Introduction

It has been known that aluminum nitride (AlN) has a wide direct-bandgap (6.2 - 5.8 eV) [1,2] with hexagonal-wurtzite crystal structure [3] and unique properties: good thermal conductivity (~3 W/cmK at 300 K) [4], good insulator (>10^{11} Ω·cm) [5], high dielectric constant [6], relatively small linear-expansion coefficients (5.3 and 4.2 × 10^{-6} K^{-1} along a- and c-axis) [7], high sound velocity (6 km/s) [8] and large hardness [9]. Owing to these properties, AlN films have potential applications to electronic devices [10], surface acoustic wave (SAW) devices [11], actuator [12], transparent hard coatings and AlN composites to light-emitting devices [13]. Also, AlN films have been used as buffer layer for GaN [14] and ZnO [15] film growth. For these applications, X-ray diffraction (XRD) technique have been extensively employed to evaluate the crystalline quality and growth orientation of AlN films which have been grown by various techniques, chemical-vapor atomic-layer deposition (a special type of CVD) [2], metal organic CVD [16], molecular beam epitaxy [17], ion beam enhanced deposition (electron beam evaporation of Al combined with N ion bombardment) [5], reactive radio-frequency (RF) magnetron sputtering deposition [6,10,18], pulsed laser deposition (PLD) [19] on various substrates, sapphire [2,19], Si [5,14-16,18], SiC [17], Al [6], Mo [12] etc. For AlN films grown on Si(111), the authors have shown that oxygen impurities near the substrate surface affect the growth orientation and suggest that the XRD intensity decreases with increasing the stress and nearly diminishes when the stress exceeds 2%, irrespective of the film thickness (27 - 470 nm) [20]. Here, the stress is defined as the difference of the lattice parameters between film and bulk. Use of the stress can be justified based on the fact that c-axis length increases with the residual-stress [18] and temperature dependence of the lattice parameter is similar to that of the residual-stress in terms of pressure [19]. The result does not agree with the lattice relaxation around 50 nm of AlN on SiC [17] and favors the constant stress throughout the AlN film on Si(111) [16]. It is of interest to study whether the suggested stress is useful for the quality evaluation of AlN film grown on different substrates other than Si(111).

In this paper, we have grown AlN on R-plane cut sapphire (R-Al_2O_3), SiO_2-glass and C-plane cut sapphire (C-Al_2O_3) substrates by a reactive RF-sputter deposition method. We have measured XRD, the composition, thick-

ness and impurities, and examined use of the stress for the film quality evaluation. We also have measured surface morphology (grain size, shape and surface smoothness), which may affect the crystalline quality, since films are polycrystalline, and optical absorption. These properties might be important for applications mentioned above. For AlN on R-Al_2O_3, irradiation with high-energy (90 MeV Ni) ions was performed in order to study whether stress relaxation, surface smoothing and bandgap modification occur or not by ion irradiation.

2. Experimental

AlN films were grown on R-Al_2O_3, SiO_2-glass and C-Al_2O_3 substrates by using a reactive-RF-sputter-deposition method with Al target (purity of 99.999%) in pure N_2 gas of ~0.3 Pa with a method described in [20,21]. A reason for usage of pure N_2 gas is to avoid Ar inclusion into films, considering that conventionally Ar and N_2 mixture gas has been employed. The substrates were subjected to ultrasonic rinse in ethanol prior to the film deposition. XRD with Cu-kα radiation was performed to examine crystalline quality and orientation. The thickness, composition and impurities of films were analyzed by RBS. The growth rate was obtained to be approximately 3 nm/min for AlN on three substrates used in this study. Light impurities such as carbon and oxygen near the film surface were analyzed by using nuclear reaction analysis (NRA), $^{12}C(d, p)^{13}C$ and $^{16}O(d, \alpha)^{14}N$ with 1.2 MeV d at the reaction angle of 160˚ [20]. In RBS and NRA, stopping powers are taken after [22] with the AlN density of 3.26 g·cm^{-3} (4.8×10^{22} Al cm^{-3}). Surface morphology was observed by atomic force microscopy (AFM) and optical absorption was measured by using a conventional spectrometer. Irradiation with 90 MeV Ni ions was performed by using a TANDEM accelerator at Japan Atomic Energy Agency at Tokai.

3. Results and Discussion

3.1. Characterization

Figure 1 shows XRD patterns and rocking curves of AlN film on R-Al_2O_3, SiO_2 and C-Al_2O_3 substrate. The substrate temperature T_s was optimized, 150˚C, 200˚C and 200˚C for these substrates, respectively so that the XRD peak intensity is maximized and the full-width at half-maximum (FWHM) of XRD rocking curve is minimized. It is found that AlN film has exceptionally a-axis, *i.e.*, (110) orientation on R-Al_2O_3 (diffraction angle $2\theta \approx 59^\circ$), in contrast to c-axis ($2\theta \approx 36^\circ$), *i.e.*, (001) orientation grown on other substrates, Si, SiO_2, C-Al_2O_3 etc. FWHM of the rocking curve of as-deposited film on R-Al_2O_3 is order of 2˚ (**Figure 1(a)** and **Table 1**). AlN on SiO_2 glass-substrates has (001) orientation and FWHM is much larger (~10˚) (**Figure 1(b)** and **Table 2**). FWHM

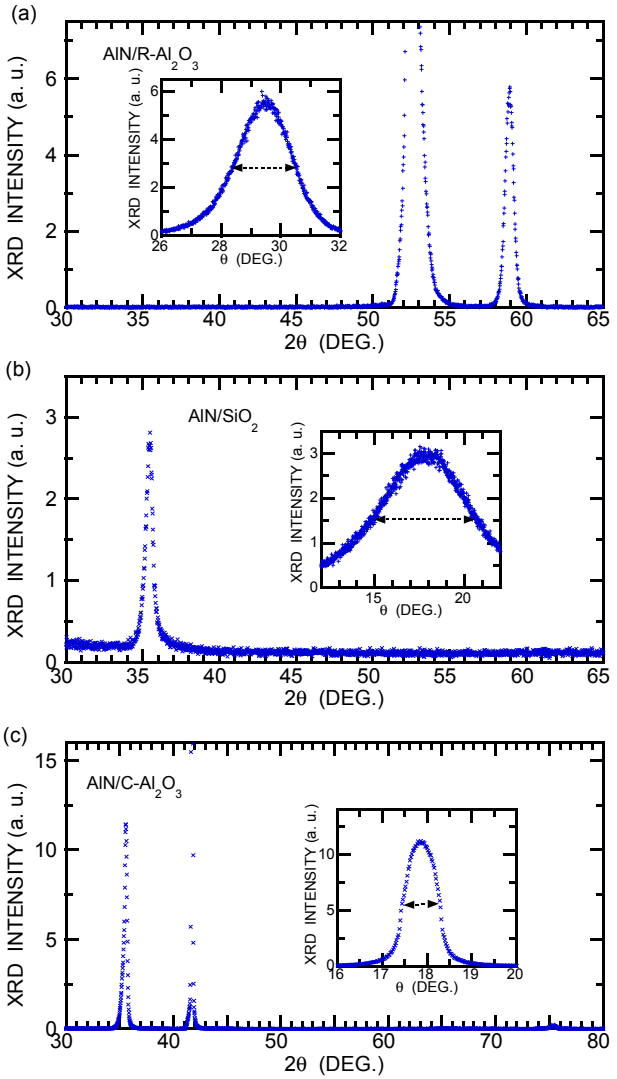

Figure 1. XRD patterns of as-deposited AlN film on R-Al_2O_3 (a), SiO_2 (b) and C-Al_2O_3 (c) substrates. Rocking curves of as-deposited films are shown in the inset and FWHM is indicated by horizontal lines. Deposition time was 55, 30 and 30 min for AlN on R-Al_2O_3, SiO_2 (sample 70c in Table 2) and C-Al_2O_3. Peaks at $2\theta \approx 59^\circ$ and 36˚ are (110) and (002) diffraction of AlN, and 52.5˚ and 41.7˚ R- and C-plane of sapphire.

of the rocking curve of as-deposited film on C-Al_2O_3 is order of 0.5˚ (**Figure 1(c)**). Hence, the crystalline quality of AlN on SiO_2-glass is poorer than that on R-Al_2O_3 and is the best for AlN on C-Al_2O_3. For AlN on C-Al_2O_3 used in this study, deposition time was 10 to 65 min or the film thickness ~30 to 200 nm.

A typical RBS of AlN on R-Al_2O_3 is shown in **Figure 2**. Similar RBS spectra were obtained for AlN on SiO_2 and C-Al_2O_3. The film thickness was deduced from the N-width illustrated in **Figure 2**. The thickness derived from RBS and XRD results are summarized in **Tables 1** and **2** for AlN on R-Al_2O_3 and SiO_2. Here, accuracies of

Table 1. A summary of RBS (thickness, L) and XRD (intensity, FWHM and a-axis length) characterization of as-deposited AlN films on R-Al_2O_3.

Sample	Deposition Time (min)	L (nm)	Relative Intensity	FWHM (deg.)	a-axis length (nm)
Z1d	15	42.7	0.85	2.68	0.3149
78b	30	95	0.002		
71a	30	115	3.2	2.22	0.3157
C3d	45	148	4.4	2.14	0.3147
95c	55	171	1.0	2.81	0.3189
X6a	67	200	2.5	2.34	0.3177
98a	55	208	8.5	2.0	0.3149
X8h	100	271	5.2	2.33	0.3170
C0f	120	368	0.79	3.7	0.3214
Y6c	160	449	10.6	2.18	0.3124

Table 2. A summary of RBS (thickness, L) and XRD (intensity, FWHM and c-axis length) characterization of as-deposited AlN films on SiO_2.

Sample	Deposition Time (min)	L (nm)	Relative Intensity	FWHM (deg.)	c-axis length (nm)
Z0c	15	37.7	0.01		
70c	30	108	2.7	6.0	0.50764
Z6e	45	148	0.54	10	0.50887
96a	55	167	0.32	16	0.51039
85h	60	184	0.08		0.50699
85c	60	190	0.07		0.50754
Y1d	65	199	1.8	8.1	0.50685
89f	56	213	0.97	9.3	0.50936
Z5e	80	233	0.016		
Y5a	100	325	2.5	8.8	0.50866

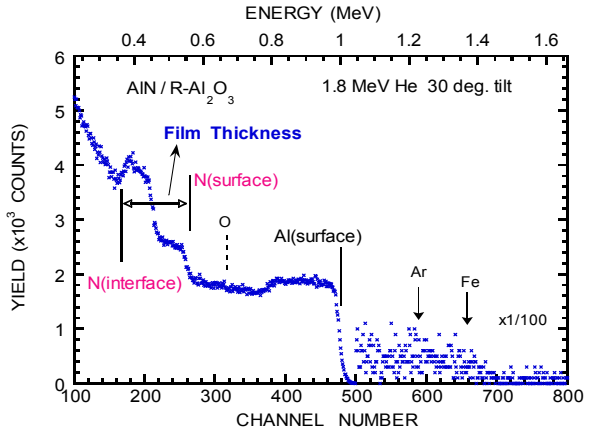

Figure 2. RBS of AlN on R-Al_2O_3 (sample 98a in Table 1). The spectra were obtained using 1.8 MeV He, and incident and outgoing angle are 30° and 50° measured from surface normal. Energies of He scattered from Al and N located at surface and interface are indicated by vertical lines. Ar and Fe impurities are also indicated.

thickness, XRD intensity, FWHM and axis length are estimated to be 10%, 20%, 3% and 0.3%, respectively. The composition appears to be nearly stoichiometric (N:Al = 1:1), within the RBS accuracy of 10%. One sees some impurities in the RBS spectra and tentatively identified as Fe (main component of stainless steel) and Ar, considering that stainless steel is the main material of RF-sputter deposition chamber and Ar gas has been often employed. We find that for 16 AlN films on R-Al_2O_3 including those given in **Table 1**, Fe and Ar impurity concentration relative to Al concentration ranges from 0.04% - 0.1% and 0.045% - 0.14%, respectively. Slightly larger amounts (Fe: 0.05% - 0.17%, and Ar: 0.4% - 0.17%) were observed for AlN on SiO_2. Similar amounts of Ar and Fe impurities were detected for AlN on C-Al_2O_3. No noticeable relation is found between the Fe impurity concentration and the XRD intensity, and between the Ar impurity concentration and the XRD intensity. NRA was performed for the films on R-Al_2O_3 given in **Table 1** and shows that the areal density of C (no information of depth profile is available because of poor depth resolution of the NRA) on/in AlN films ranges from 5 to 18 × 10^{15} cm^{-2}, larger than ~3 × 10^{15} cm^{-2} for virgin R-Al_2O_3 substrate. NRA also shows that the areal density of O near the film surface ranges from 8 - 16 × 10^{15} cm^{-2}. Similar amounts of C and O were detected for

AlN on SiO_2 (C: 7 to 15 × 10^{15} cm^{-2}, O near the film surface: 6 to 17 × 10^{15} cm^{-2}). Again no clear relation is observed between the XRD intensity and C impurity density, and between the XRD intensity and O impurity density near the film surface. The former result leads to a speculation that the majority of C impurities are located near the surface. For AlN on C-Al_2O_3, similar amounts of impurities are assumed.

One sees that the XRD intensity does not follow a linear increase with the film thickness for AlN on R-Al_2O_3 and SiO_2 (**Tables 1** and **2**) and the similar situations is observed for AlN on C-Al_2O_3. As suggested in [20], XRD intensity vs stress is shown in **Figure 3**. Here, the stress is defined by the axis length of the film divided by the bulk value (0.31111 and 0.49788 nm for a- and c-axis [23]) minus unity, assuming that the stress defined above represents the residual-stress as mentioned earlier. Usually, several samples were prepared in the same run. For a particular run for AlN on R-Al_2O_3, having the film thickness around 380 nm, the results of four samples are shown. Accidentally, the sample (C0f) given in **Table 1** is the poorest in the crystalline quality (XRD intensity is the lowest). As shown in **Figure 3**, it is found that the XRD intensity decreases with increasing the stress, except for the thinnest films, regardless of the substrates, as observed for AlN with c-axis orientation on Si(111) substrate [20]. These results indicate no relaxation of the stress regardless of the film thickness and substrates, implying that the stress is an import factor determining the crystalline quality, and that a simple explanation by misfit (lattice parameter mismatch between the film and substrate) is not applicable to the present results. Introduction of the stress might be affected by O, C and possibly H impurities in the film as well as substrate surface condition, and these are to be investigated.

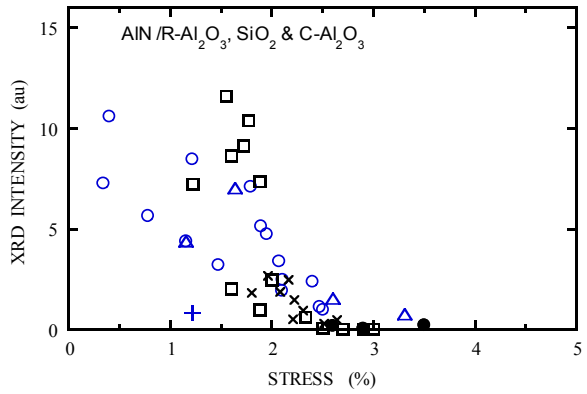

Figure 3. XRD intensity vs stress for AlN films on R-Al_2O_3 (O, Δ, +), SiO_2 (x) and C-Al_2O_3 (□, ●). Data (Δ) are taken for the films prepared in the same run having the thickness of ~380 nm. Datum indicated by + is the result of the thinnest film (sample of Z1d in Table 1). For AlN on C-Al_2O_3, film thickness is less than 50 nm (●) and 90 - 200 nm (□).

3.2. Surface Morphology, Optical Absorption and High-Energy Ion Irradiation Effects

Surface morphology is mainly studied for AlN on R-Al_2O_3 and SiO_2. An AFM image of as-deposited AlN film on R-Al_2O_3 is shown in **Figure 4(a)**. One sees that a column with c-axis orientation lays down parallel to the surface. The grain is often non-spherical, columnar and thus the grain size is less well-defined. It appears that the smaller size of columnar grains ranges from 20 to 40 nm and their length extends to over 250 nm, as shown in **Figure 5(a)** and surface smoothness (or roughness) in terms of root mean square (RMS) of the surface height ranges from 0.2 - 3 nm as shown in **Figure 5(b)**. It appears that surface roughness increases linearly with the film thickness for AlN on R-Al_2O_3. **Figure 4(b)** shows an AFM image of AlN film on R-Al_2O_3 after irradiation of 90 MeV Ni ions at 1 × 10^{13} cm^{-2}, and ion irradiation effects will be described later. **Figures 4(c)** and **(d)** show AFM images of AlN on SiO_2 and C-Al_2O_3 and cross section of grains on these substrates is nearly circular. The grain size of AlN on SiO_2 is 10 - 40 nm (**Figure 5(a)**) and RMS is 0.8 - 2 nm (**Figure 5(b)**). Grain size is ~20 nm for AlN on C-Al_2O_3 shown in **Figure 4(d)**, where RMS is 0.36 nm. In this study, surface smoothness is the best for AlN on C-Al_2O_3 and poorest on SiO_2. For 90 MeV Ni ion irradiation on AlN on R-Al_2O_3 at 10^{13} cm^{-2}, change was not observed in RBS (see **Figure 2**) and AFM image remained nearly the same as before irradiation, but surface roughness (RMS) slightly decreases (from 0.75 nm to 0.55 nm).

For AlN on R-Al_2O_3 under irradiation with 90 MeV Ni ions up to 6 × 10^{13} cm^{-2}, which appears to cause significant inelastic-collision-effects [25], no change in the axis-length was observed within 0.1%, *i.e.*, no stress relaxation by ion irradiation and the XRD intensity at the fluence of ~6 × 10^{13} cm^{-2} decreases to half of that of as-deposited film. No appreciable but slight (several %) reduction in FWHM of the XRD rocking curve was observed at ~around 10^{13} cm^{-2}.

Optical absorption spectra of AlN on R-Al_2O_3 are shown in **Figure 6**. The bandgap as of deposited film is obtained to be 5.7 eV in reasonable agreement with the reported value of ~6.0 eV [1,2]. Optical absorption has little changed, except for the wavelength below 300 nm (**Figure 6**) and the bandgap decreases by ~0.2 eV. Similarly, the bandgap of 5.7 eV is obtained for as-deposited AlN film on SiO_2.

4. Summary

We have presented characterization of AlN films on R-Al_2O_3, SiO_2-glass and C-Al_2O_3 substrates by means of XRD, ion beam technique, AFM and optical absorption. Good quality of AlN films with exceptional orientation

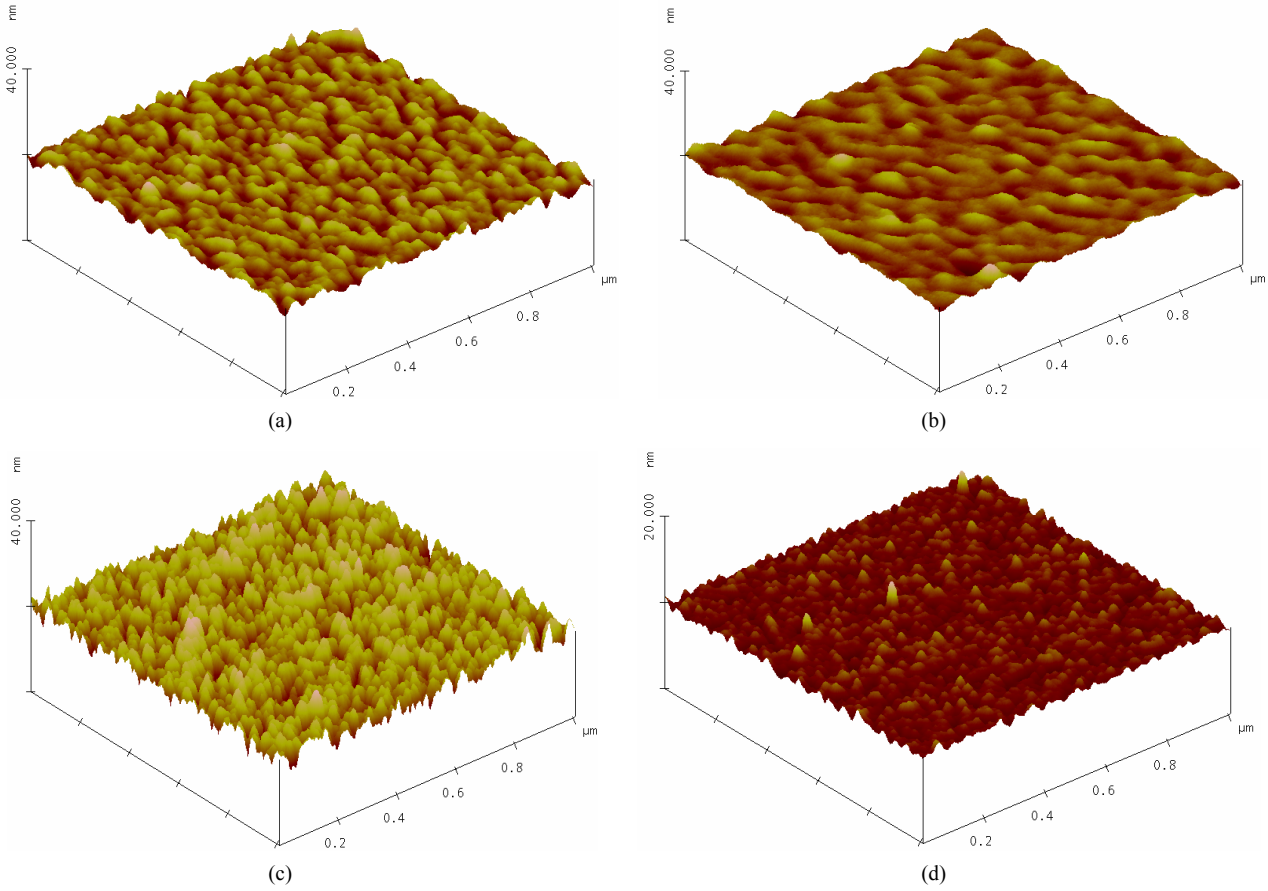

Figure 4. (a) AFM image of as-deposited AlN film on R-Al_2O_3. Deposition time was 55 min. Surface roughness (RMS) is 0.75 nm; (b) AFM image of AlN film on R-Al_2O_3 (sample shown in Figure 4(a)) after irradiation with 90 MeV Ni ions at 1 × 10^{13} cm^{-2}; (c) AFM image of as-deposited AlN film on SiO_2 (sample: 85h in Table 2). Deposition time was 60 min. Surface roughness (RMS) is 1.7 nm; (d) AFM image of as-deposited AlN film on C-Al_2O_3. Deposition time was 60 min. Surface roughness (RMS) is 0.36 nm.

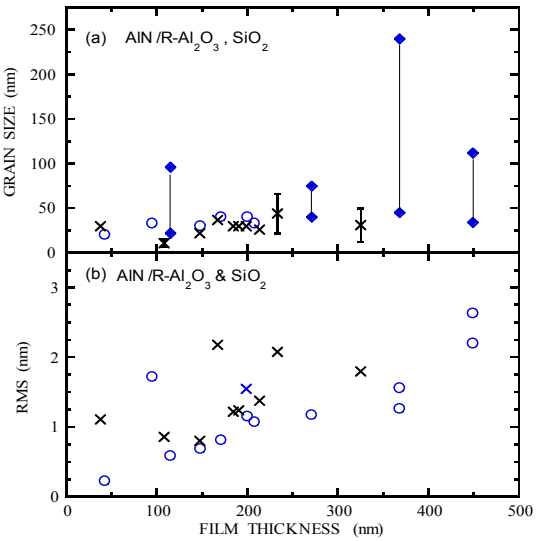

Figure 5. (a) Grain size (nm) vs film thickness (nm) for AlN on R-Al_2O_3 (O, ◆) and SiO_2 (x) and (b) surface roughness in terms of root mean square (RMS) vs film thickness for AlN on R-Al_2O_3 (O) and SiO_2 (x).

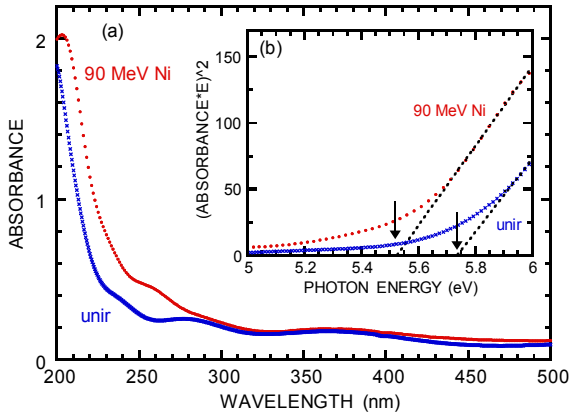

Figure 6. Optical absorption spectra before and after irradiation with 90 MeV Ni ions at 1 × 10^{13} cm^{-2}. Inset shows the square of absorbance times photon energy vs photon energy, illustrating bandgap determination.

of a-axis orientation has been obtained on R-Al_2O_3 substrate and a correlation is found between the stress and crystalline quality in terms of XRD intensity. Effects of

irradiation with 90 MeV Ni ions have been briefly described.

5. Acknowledgements

XRD was performed at EcoTopia Science Institute and Radioisotope Research Center, Nagoya University. The authors thank Mr. T. Masuda for technical assistance of ion beam analysis performed at Nagoya University.

REFERENCES

[1] W. M. Yim, E. J. Stofko, P. J. Zanzucchi, J. I. Pankove, M. Ettenberg and S. L. Gilbert, "Epitaxially Grown AlN and Its Optical Band Gap," *Journal of Applied Physics*, Vol. 44, No. 1, 1973, pp. 292-296. doi:10.1063/1.1661876

[2] C. Ozgit, I. Donmez, M. Alevli and N. Biyikli, "Self-Limiting Low-Temperature Growth of Crystalline AlN Thin Films by Plasma-Enhanced Atomic Layer Deposition," *Thin Solid Films*, Vol. 520, 2012, pp. 2750-2755. doi:10.1016/j.tsf.2011.11.081

[3] K. M. Taylor and C. Lenie, "Some Properties of Aluminum Nitride," *Journal of the Electrochemical Society*, Vol. 107, No. 4, 1960, pp. 308-314. doi:10.1149/1.2427686

[4] G. A. Slack, "Nonmetallic Crystals with High Thermal Conductivity," *Journal of Physics and Chemistry of Solids*, Vol. 34, No. 2, 1973, pp. 321-335. doi:10.1016/0022-3697(73)90092-9

[5] Z. An, C. Men, Z. Xu, P. K. Chu and C. Lin, "Electrical Properties of AlN Thin Films Prepared by Ion Beam Enhanced Deposition," *Surface & Coatings Technology*, Vol. 196, No. 1-3, 2005, pp. 130-134. doi:10.1016/j.surfcoat.2004.08.169

[6] X. Song, R. Fu and H. He, "Frequency Effects on the Dielectric Properties of AlN Film Deposited by Radio Frequency Reactive Magnetron Sputtering," *Microelectronic Engineering*, Vol. 86, No. 11, 2009, pp. 2217-2221. doi:10.1016/j.mee.2009.03.036

[7] W. M. Yim and R. J. Paff, "Thermal Expansion of AlN, Sapphire, and Silicon," *Journal of Applied Physics*, Vol. 45, No. 3, 1974, pp. 1456-1457. doi:10.1063/1.1663432

[8] S. P. Dodd, G. A. Saunders, M. Cankurtaran and B. James, "Ultrasonic Study of the Elastic and Nonlinear Acoustic Properties of Ceramic Aluminum Nitride," *Journal of Materials Science*, Vol. 36, No. 3, 2001, pp. 723-729. doi:10.1023/A:1004897126648

[9] I. Yonenaga, "Thermo-Mechanical Stability of Wide-Bandgap Semiconductors: High Temperature Hardness of SiC, AlN, GaN, ZnO and ZnSe," *Physica B*: *Condensed Matter*, Vol. 308-310, 2001, pp. 1150-1152. doi:10.1016/S0921-4526(01)00922-X

[10] A. F. Belyanin, L. L. Bouilov, V. V. Zhirnov, A. I. Kamenev, K. A. Kovalskij and B. V. Spitsyn, "Applications of Aluminum Nitride Films for Electronic Devices," *Diamond and Related Materials*, Vol. 8, No. 2-5, 1999, pp. 369-372. doi:10.1016/S0925-9635(98)00412-9

[11] M. B. Assouar, O. Elmazria, P. Kirsch, P. Alnot, V. Mortet and C. Tiusan, "High-Frequency Surface Acoustic Wave Devices Based on AlN/Diamond Layered Structure Realized Using E-Beam Lithography," *Journal of Applied Physics*, Vol. 101, 2007, Article ID: 114507. doi:10.1063/1.2739218

[12] J. Olivares, E. Iborra, M. Clement, L. Vergara, J. Sangrador and A. Sanz-Hervas, "Piezoelectric Actuation of Microbridges Using AlN," *Sensors and Actuators A*, Vol. 123-124, 2005, pp. 590-595. doi:10.1016/j.sna.2005.03.066

[13] F. A. Ponce and D. P. Bour, "Nitride-Based Semiconductors for Blue and Green Light-Emitting Devices," *Nature*, Vol. 386, 1997, pp. 351-359. doi:10.1038/386351a0

[14] X. Ni, L. Zhu, Z. Ye, Z. Zhao, H. Tang, W. Hong and B. Zhao, "Growth and Characterization of GaN Films on Si(111) Substrate Using High-Temperature AlN Buffer Layer," *Surface & Coatings Technology*, Vol. 198, No. 1-3, 2005, pp. 350-353. doi:10.1016/j.surfcoat.2004.10.073

[15] V. Venkatachalapathy, A. Galeckas, I.-H. Lee and A. Y. Kuznetsov, "Engineering of Nearly Strain Free ZnO Films on Si(111) by Tuning AlN Buffer Thickness," *Physica B*: *Condensed Matter*, Vol. 407, 2012, pp. 1476-1480. doi:10.1016/j.physb.2011.09.065

[16] S. Raghavan and J. M. Redwing, "*In Situ* Stress Measurements during the MOCVD Growth of AlN Buffer Layers on (111) Si Substrates," *Journal of Crystal Growth*, Vol. 261, No. 2-3, 2004, pp. 294-300. doi:10.1016/j.jcrysgro.2003.11.020

[17] N. Onojima, J. Suda and H. Matsunami, "Lattice Relaxation Process of AlN Growth on Atomically Flat 6H-SiC Substrate in Molecular Beam Epitaxy," *Journal of Crystal Growth*, Vol. 237-239, 2002, pp. 1012-1016. doi:10.1016/S0022-0248(01)02118-2

[18] S.-H. Lee, K. H. Yoon, D.-S. Cheong and J.-K. Lee, "Relationship between Residual Stress and Structural Properties of AlN Films Deposited by r.f. Reacrive Sputtering," *Thin Solid Films*, Vol. 435, No. 1-2, 2003, pp. 193-198. doi:10.1016/S0040-6090(03)00353-5

[19] J. Keckes, S. Six, W. Tesch, R. Resel and B. Rauschenbach, "Evaluation of Thermal and Growth Stresses in Heteroepitaxial AlN Thin Films Formed on (0001) Sapphire by Pulsed Laser Ablation," *Journal of Crystal Growth*, Vol. 240, No. 1-2, 2002, pp. 80-86. doi:10.1016/S0022-0248(02)00877-1

[20] N. Matsunami, S. Venkatachalam, M. Tazawa, H. Kakiuchida and M. Sataka, "Ion Beam Characterization of rf-Sputter Deposited AlN Films on Si(111)," *Nuclear Instruments Methods B*, Vol. 266, No. 8, 2008, pp. 1522-1526. doi:10.1016/j.nimb.2007.12.086

[21] N. Matsunami, T. Shimura, M. Tazawa, T. Kusumori, H. Kakiuchida, M. Ikeyama, Y. Chimi and M. Sataka, "Modifications of AlN Thin Films by Ions," *Nuclear Instruments Methods B*, Vol. 257, No. 1-2, 2007, pp. 433-437. doi:10.1016/j.nimb.2007.01.043

[22] J. F. Ziegler, J. P. Biersack and U. Littmark, "The Stopping and Range of Ions in Solids," Pergamon Press, New York, 1985.

[23] W. Martienssen and H. Warlimont, "Handbook of Condensed Matter and Materials Data," Springer, Berlin, 2005. doi:10.1007/3-540-30437-1

[24] J. X. Zhang, H. Cheng, Y. Z. Chen, A. Uddin, S. Yuan, S. J. Geng and S. Zhang, "Growth of AlN Films on Si(100) and Si(111) Substrates by Reactive Magnetron Sputtering," *Surface Coating & Technology*, Vol. 198, No. 1-3, 2005, pp. 68-73. doi:10.1016/j.surfcoat.2004.10.075

[25] N. Matsunami, M. Sataka, S. Okayasu and M. Tazawa, "Electronic Sputtering of Nitrides by High-Energy Ions," *Nuclear Instruments Methods B*, Vol. 256, No. 1, 2007, pp. 333-336. doi:10.1016/j.nimb.2006.12.022

